Appendix 1:
Age-prevalence curves in a multi-species parasite community

Daniel L. Preston, Landon P. Falke, Mark Novak

Table S1. Generalized additive model (GAM) results for the effect of host size on infection status (zero or one). Separate models were run for infection by any trematode ('All taxa combined') and for each of the eight taxa separately. The effective degrees of freedom provides a measure of the degree of non-linearity in the host size predictor, with values above 2 being strongly non-linear.

Taxon	Effective Degrees of Freedom	Test Statistic (Chi-Square)	p-value
All taxa combined	5.2	1383	< 0.0001
M. oregonensis	3.7	499	< 0.0001
N. salmincola	1.0	179	< 0.0001
A. oregonense	6.4	154	< 0.0001
Metagonimus sp.	5.3	836	< 0.0001
Stephanoprora sp.	1.7	86	< 0.0001
C. alseae	1.6	25	< 0.0001
D. aspina	2.9	30	< 0.0001
P. siliculus	2.7	8.8	0.05

Table S2. Aikaike Information Criterion (AIC) values for generalized additive models (GAMs) comparing models with only an effect of host body size to models with an interaction between host body size and the prevalence of other potentially interacting trematodes. Models include infection status (zero or one) as the binomial response for the trematodes listed at the far left under 'Response Taxon'.

Response Taxon	Model Structure	AIC
Metagonimus sp.	Size	6943.2
	Size**M. oregonensis*	6927.2
	Size**N. salmincola*	6895.7
	Size**A. oregonense*	6848.0
M. oregonensis	Size	2974.7
	Size**N. salmincola*	2871.7
	Size**A. oregonense*	2963.5
	Size**Metagonimus sp.*	2920.1
A. oregonense	Size	9400.2
	Size**M .oregonensis*	9306.1
	Size**N. salmincola*	9327.9
	Size**Metagonimus*	9228.7
N. salmincola	Size	6682.8
	Size**M .oregonensis*	6450.2
	Size**A. oregonense*	6590.7
	Size**Metagonimus sp.*	6473.5
D. aspina	Size	2220.8
	Size**M .oregonensis*	2216.9
	Size**Metagonimus sp.*	2210.3
	Size**N. salmincola*	2211.3
	Size**A. oregonense*	2125.7
P. siliculus	Size	1662.8
	Size**M .oregonensis*	1664.9
	Size**Metagonimus sp.*	1658.9
	Size**N. salmincola*	1668.4
	Size**A. oregonense*	1655.8
C. alseae	Size	252.9
	Size**M .oregonensis*	250.7
	Size**Metagonimus sp.*	252.7
	Size**N. salmincola*	254.1
	Size**A. oregonense*	245.0
Stephanoprora sp.	Size	925.0
	Size**M .oregonensis*	911.8
	Size**Metagonimus sp.*	887.9
	Size**N. salmincola*	926.6
	Size**A. oregonense*	904.9

Table S3. Body size and pharynx measurements recorded using image analysis of freshly isolated trematodes from *Juga* host snails in single infections. Body measurements correspond to the sporocyst stage if the taxon lacks a redia stage (indicated by the second column); otherwise body measurements correspond to the redia stage. Pharynx diameter is not applicable to taxa with only sporocyst stages. Photos were taken at 10X magnification and trematodes were measured using ImageJ software. Each set of measurements represents an average from two to four mature individual trematode larvae, which had very little variance in their body size measurements across individuals.

Taxon	Stage	Maximum Body length (mm)	Maximum body width (mm)	Pharynx diameter (mm)
M. oregonensis	redia	1.57	0.33	0.04
N. salmincola	redia	1.8	0.38	0.08
A. oregonense	sporocyst	0.38	0.28	NA
Metagonimus sp.	redia	1.28	0.12	0.04
Stephanoprora sp.	redia	1.07	0.34	0.09
C. alseae	sporocyst	0.17	0.11	NA
D. aspina	redia	1.8	0.36	0.07
P. siliculus	sporocyst	3.03	0.61	NA

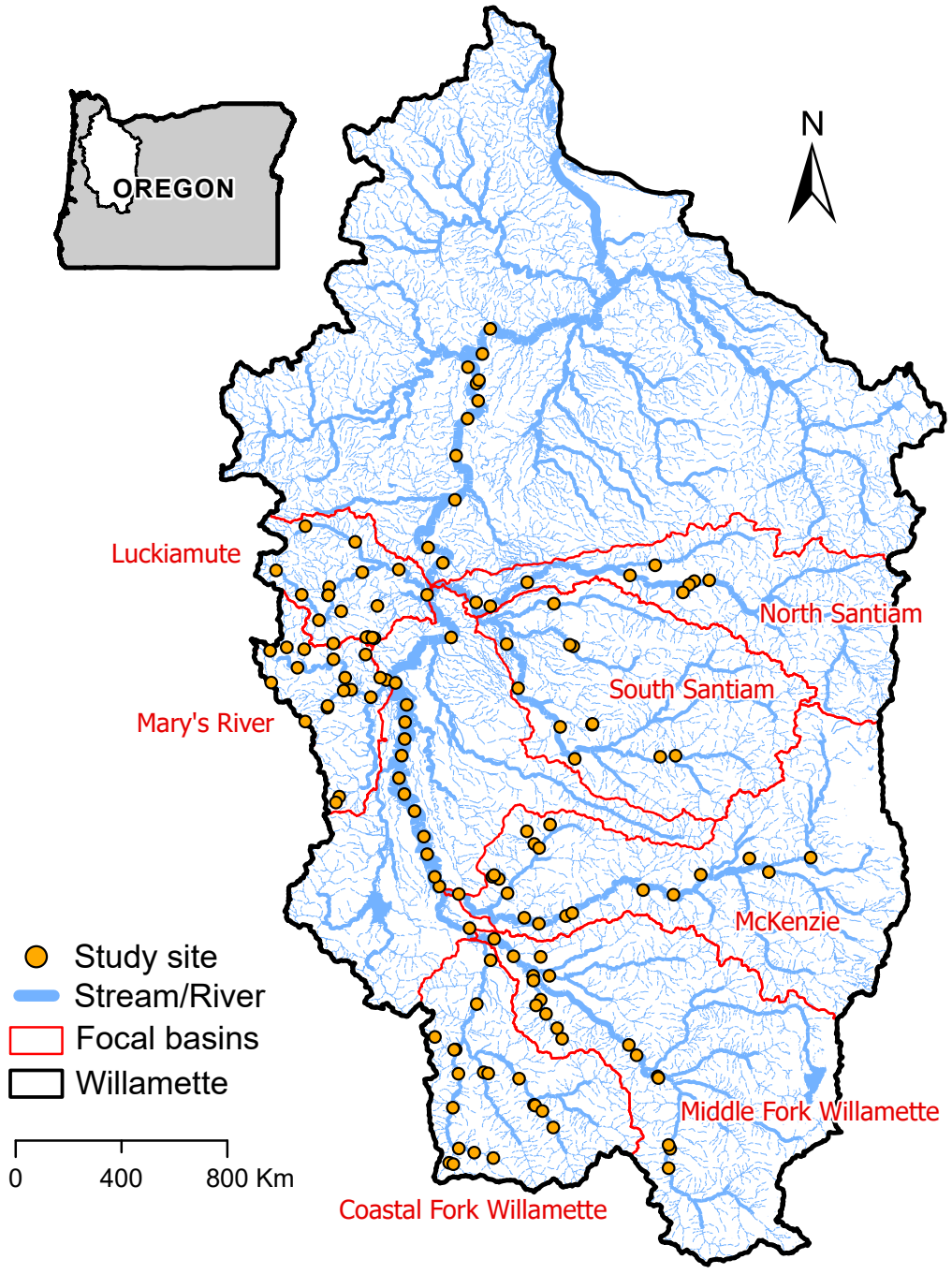

Fig. S1. Site map showing sampling locations within the Willamette Valley, Oregon, USA. Twenty-five of the sites were on the mainstem Willamette River and 18 to 20 sites were within each of six Willamette tributaries, including the Santiam, McKenzie, Middle Fork Willamette, Coast Fork Willamette, Mary's, and Luckiamute Rivers.

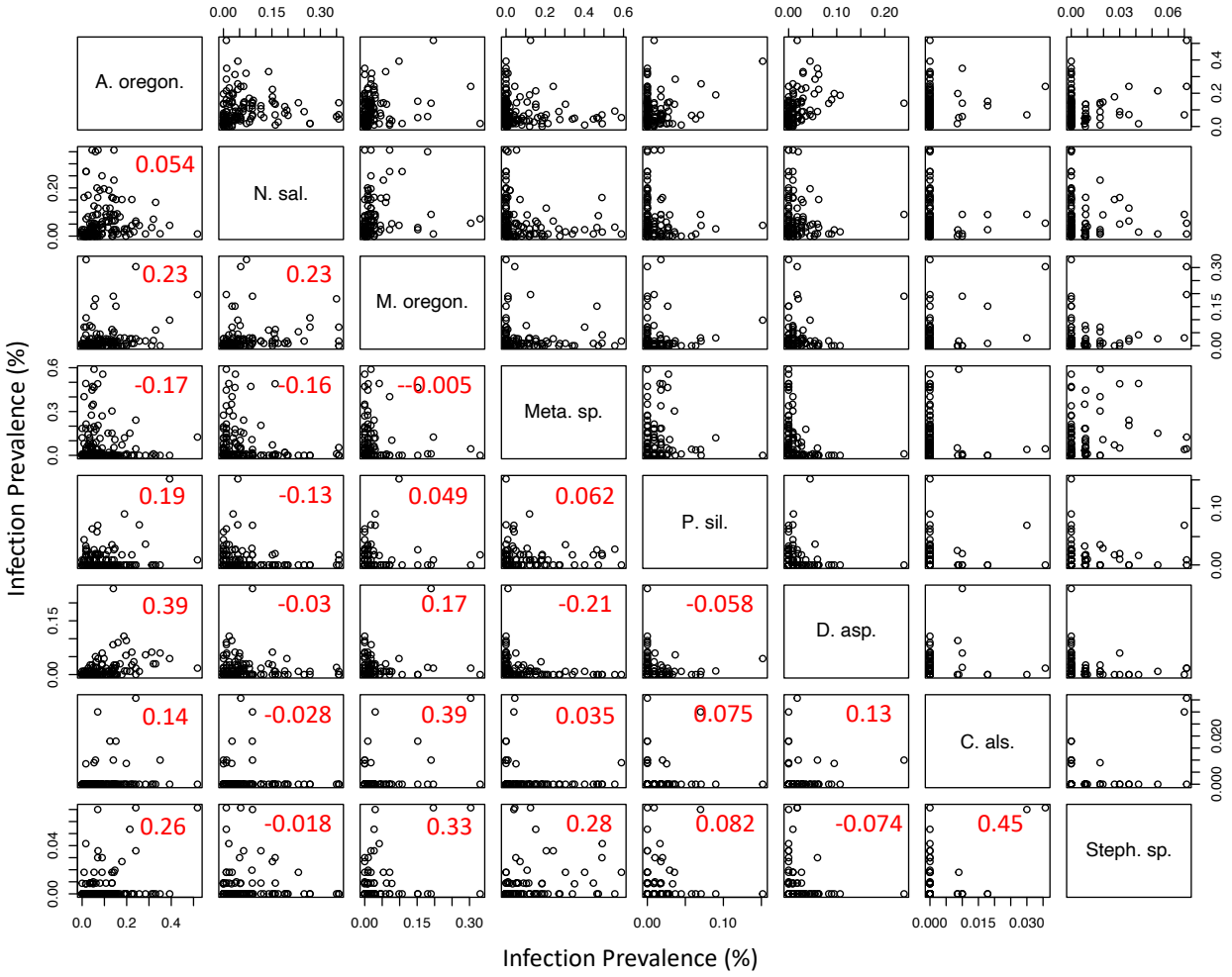

Figure S2. Correlations between the site-level prevalences of eight trematode taxa. The numbers in red show the Pearson correlation coefficients. Data are from 137 sites surveys in the Willamette River watershed in western Oregon, USA. The top left four taxa are the focal taxa used to investigate interactions between trematodes. Note the differences in the y-axes across panels. The taxon abbreviations are as follow: "A. oregon." = *Acanthatrium oregonense*, "N. sal." = *Nanophyetus salmincola*, "M. oregon." = *Metagonimoides oregonensis*, "Meta. sp." = *Metagonimus* sp., "P. sil." = *Plagioporus siliculus*, "D. asp." = *Deropegus aspina*, "C. als." = *Cardicola alseae*, and "Steph. sp." = *Stephanoprora* sp.

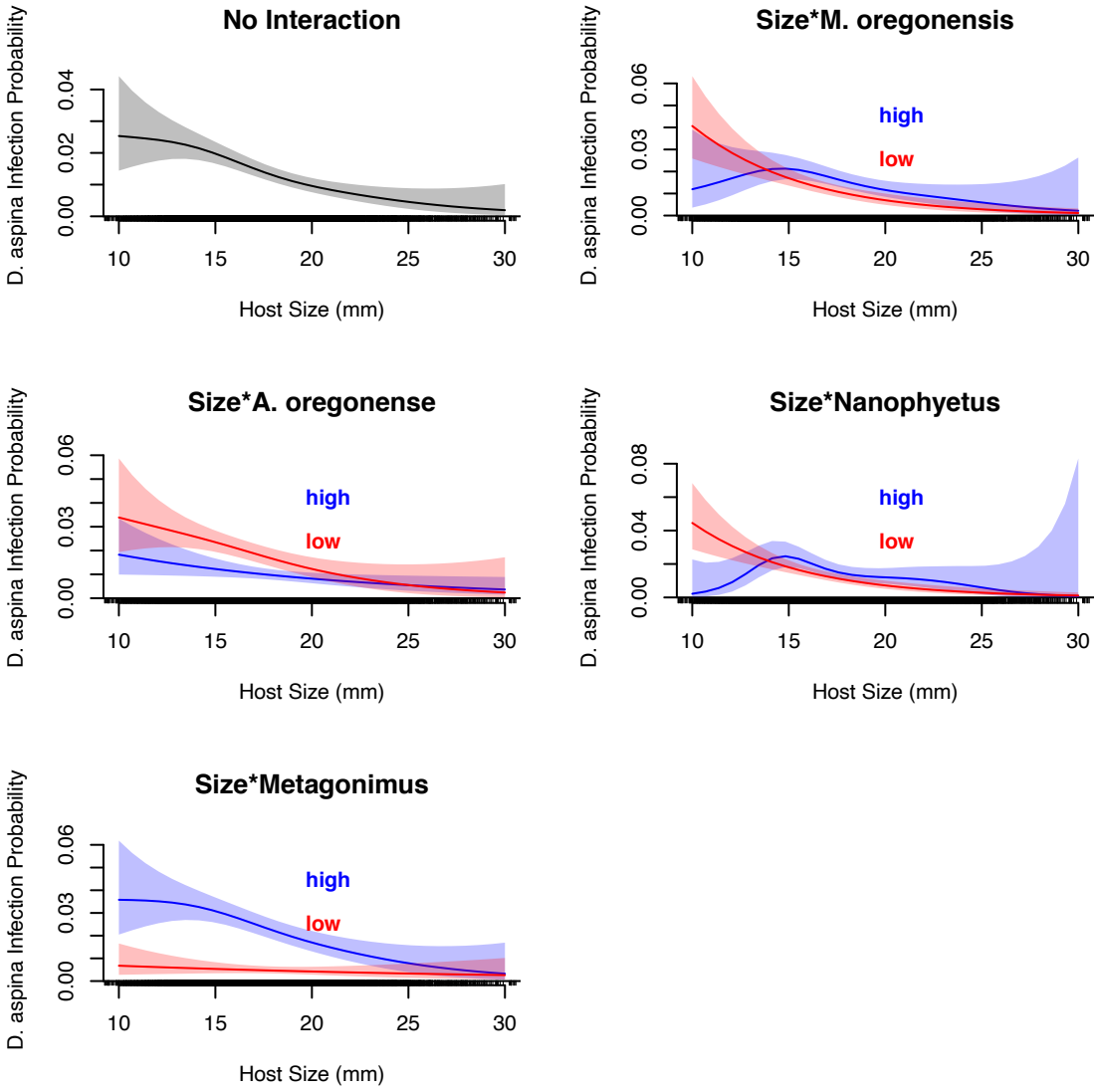

Figure S3. Partial effects plots for the effects of host size on infection probability by *Deropegus aspina*. The plots show results from a model with only host size, and models with interactions between host size and four other of the most abundant trematodes (*Metagonimoides oregonensis*, *Acanthatrium oregonense, Nanophyetus salmincola*, and *Metagonimus* sp.). For models with interactions, the curve in blue reflects the high prevalence of the potentially interacting trematode and the curve in red reflects the low prevalence of the potentially interacting trematode. The response trematode is shown the y-axis label. The values have been transformed from the logit scale to indicate infection probabilities. The shaded areas are 95% confidence bands. Note differences in the y-axis scale.

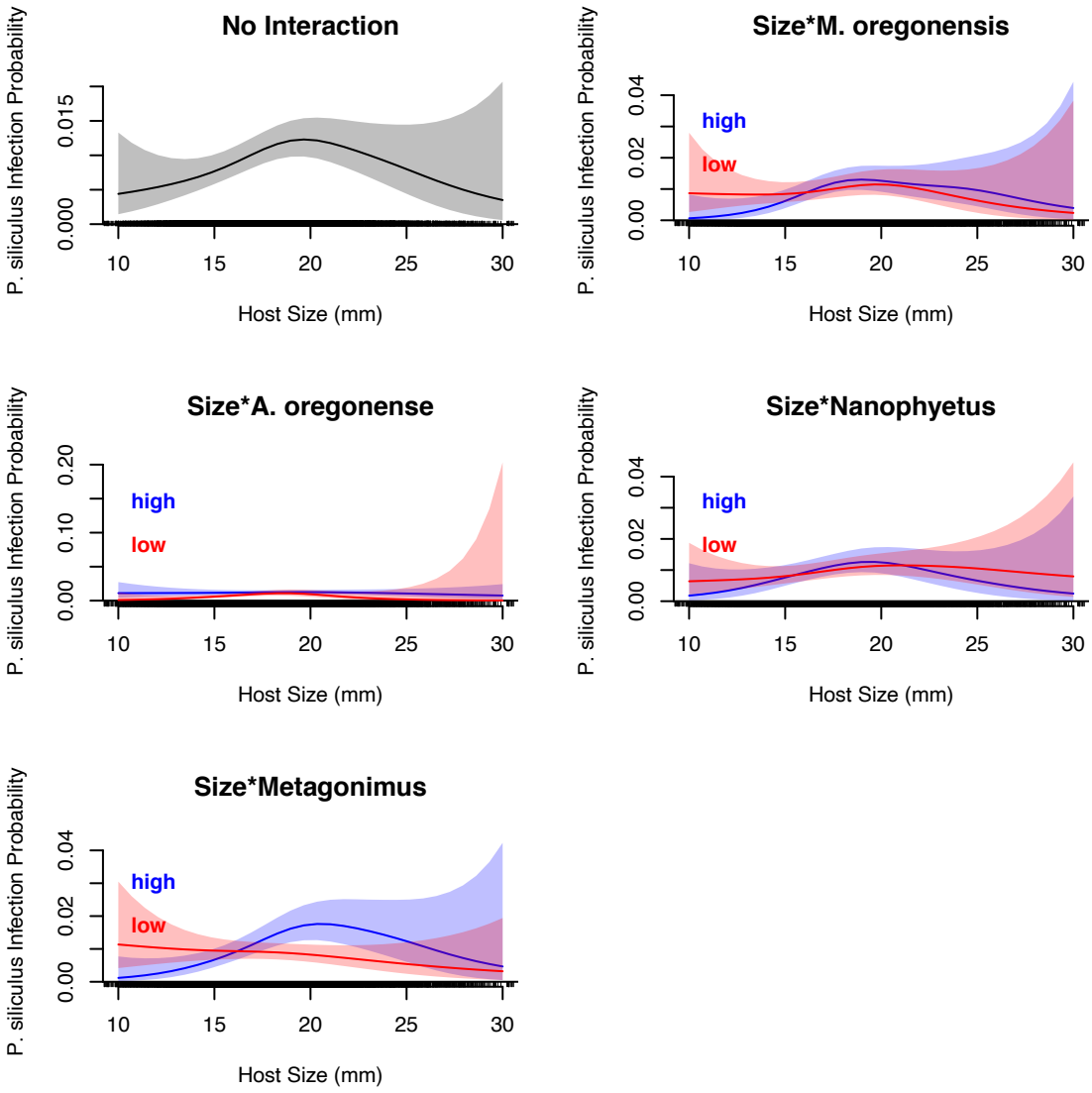

Figure S4. As in Fig. S3 but for *Plagioporus siliculus* as the focal taxon.

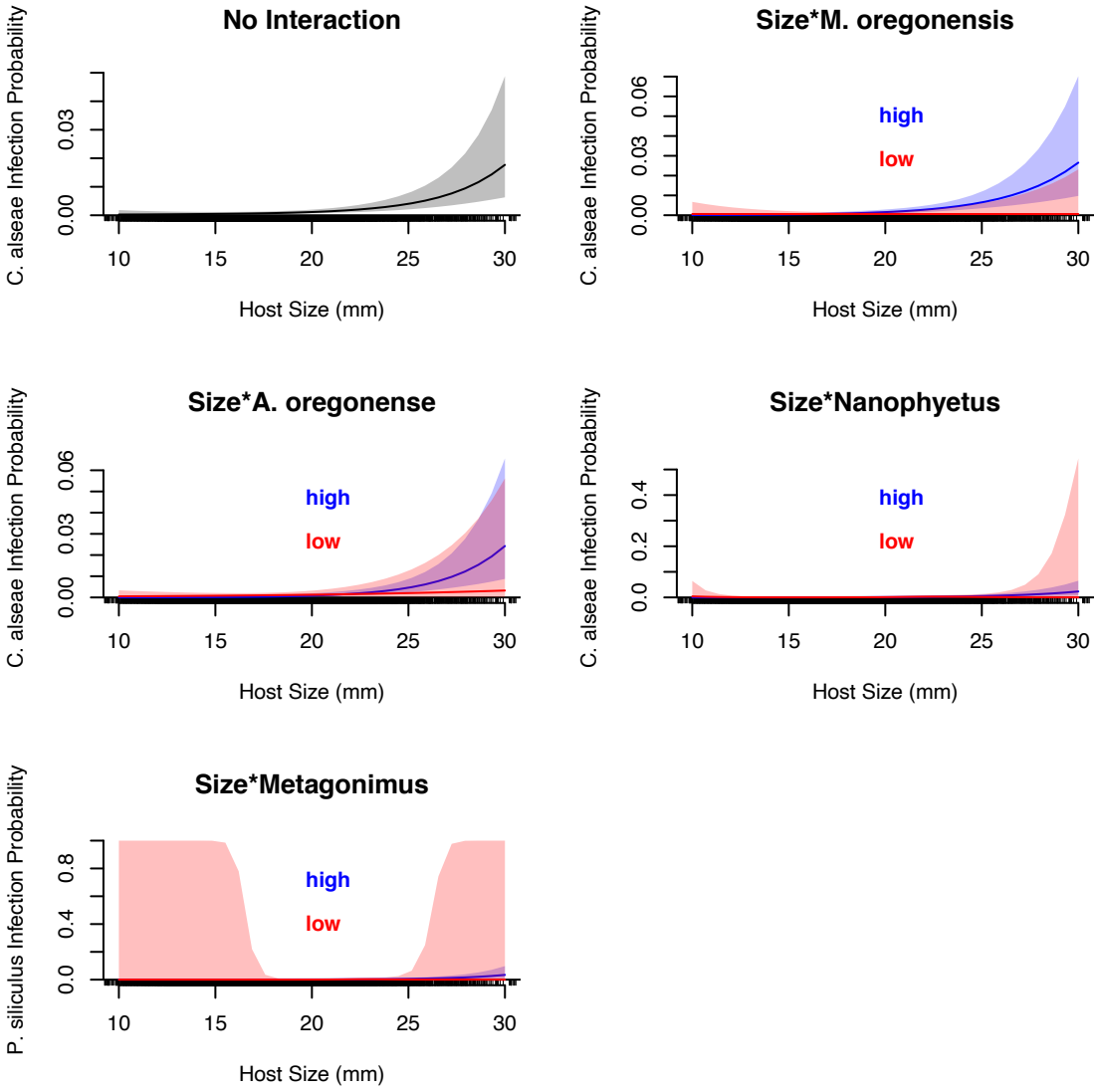

Figure S5. As in Fig. S3 but for *Cardicola alseae* as the focal taxon.

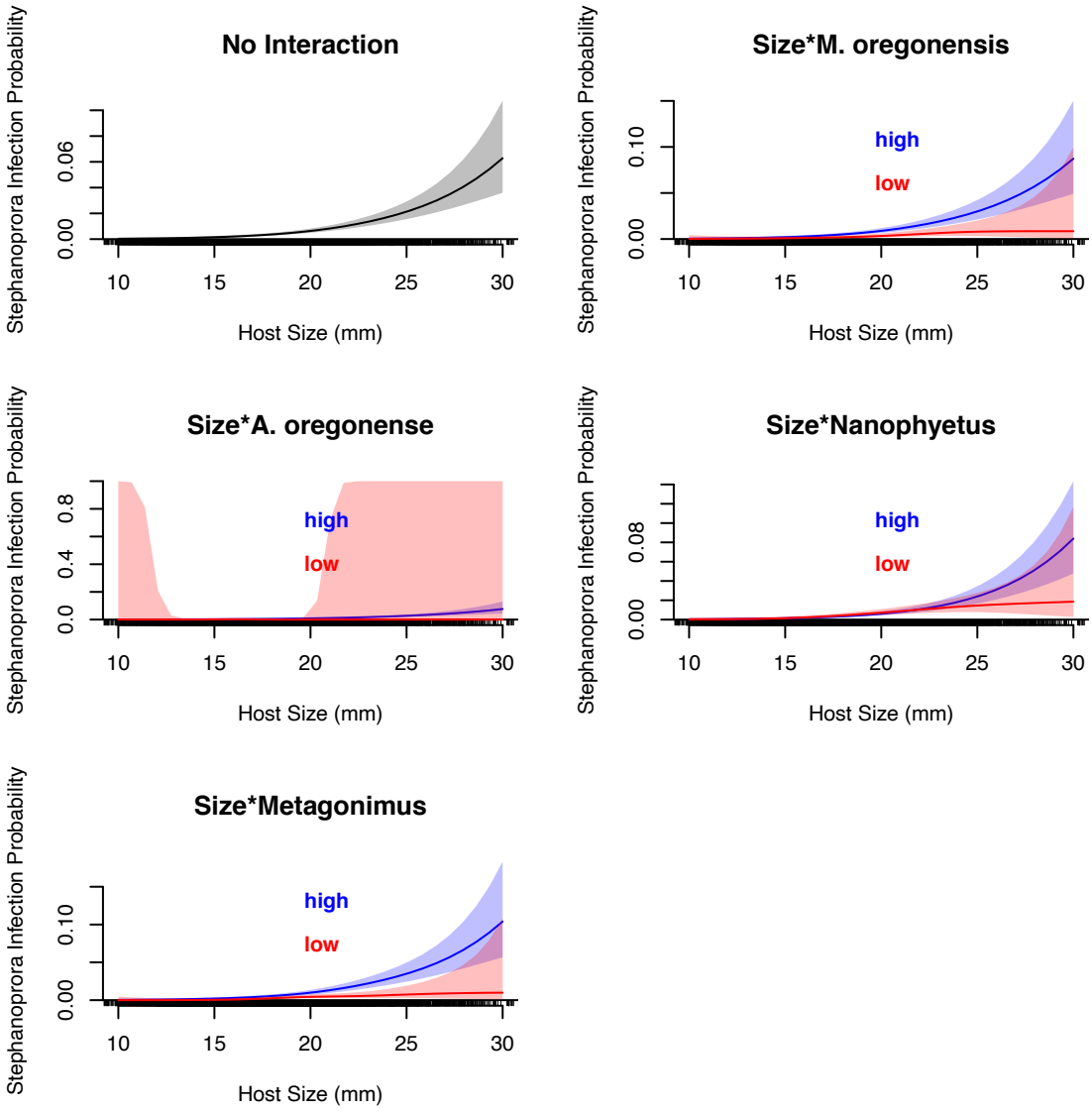

Figure S6. As in Fig. S3 but for *Stephanoprora* sp. as the focal taxon.

Appendix 2:
Age-prevalence curves in a multi-species parasite community

Daniel L. Preston, Landon P. Falke, Mark Novak

The model considered in the main text describes the density dynamics of uninfected hosts $x(t)$, hosts infected by a dominant parasite $y(t)$, and hosts infected by subordinate parasite $z(t)$ as a three-variable system of *ordinary* differential equations. Starting from an initial state in which all hosts are uninfected, the model represents a cohort of equal-aged individuals who die and acquire infections as time (and hence individual age) advances. We therefore equate time and age when assessing how variation in the force-of-infection and infection-induced mortality affect the age-prevalence curves of the two parasite species. In this appendix, we demonstrate that equivalent age-prevalence curves are obtained at the long-term steady-state when time and age are considered to be distinct. We do so by approximating a system of *partial* differential equations wherein individuals not only die and become infected as they age but also produce new age-0 individuals (that die and become infected as they age) over time. This second model can therefore characterize changes in the shapes of the two parasites' age-prevalence curves over time.

Lotka-McKendrick model

The starting point for our model is the Lotka-McKendrick demographic model which describes the dynamics of a single age-structured population . With $x(a,t)$ being the density of individuals of age a at time t, $x(0,t)$ being the density of age-0 individuals born at time t, $\mu(a)$ being the mortality rate of individuals of age a, and $f(a)$ being the fertility rate of individuals of age a,

the model may be written as

$$\frac{\partial x(a,t)}{\partial a} + \frac{\partial x(a,t)}{\partial t} = -\mu(a)\; x(a,t) \tag{S1a}$$

$$x(0,t) = \int_0^{a_+} x(a,t)\; f(a)\; da \tag{S1b}$$

$$x(a,0) = x_d(a)\,, \tag{S1c}$$

where $x_d(a)$ is the initial age distribution of the population at time 0 and a_+ is the maximum possible age. Although the atypical boundary condition $x(0,t)$ of this model — describing the rate at which age-0 individuals enter the population — makes the solution to this partial differential equation model analytically intractable, several approximating techniques exist of which we employ one (see below).

Extension to two-parasite model

We extend model (S1) to consider not only the $x(a,t)$ density of (uninfected host) individuals but also the $y(a,t)$ density of hosts infected by a dominant parasite and the $z(a,t)$ density of hosts infected by a subordinate parasite:

$$\frac{\partial x(a,t)}{\partial a} + \frac{\partial x(a,t)}{\partial t} = -\mu_x(a)\; x(a,t) - \lambda_y(a)\; x(a,t) - \lambda_z(a)\; x(a,t) \tag{S2a}$$

$$\frac{\partial y(a,t)}{\partial a} + \frac{\partial y(a,t)}{\partial t} = -\mu_y(a)\; y(a,t) + \lambda_y(a)\; x(a,t) + \lambda_y(a)\; z(a,t) \tag{S2b}$$

$$\frac{\partial z(a,t)}{\partial a} + \frac{\partial z(a,t)}{\partial t} = -\mu_z(a)\; z(a,t) + \lambda_z(a)\; x(a,t) - \lambda_y(a)\; z(a,t)\,. \tag{S2c}$$

Here $\lambda_y(a)$ and $\lambda_z(a)$ are the parasites' respective age-specific force-of-infection rates and the age-specific mortality rates, $\mu_u(a)$, $\mu_y(a)$, and $\mu_z(a)$, may differ between the three groups of individuals. As boundary conditions we consider

$$x(0,t) = \int_0^{\infty} x(a,t)\; f_x(a)\; da \tag{S2d}$$

$$y(0,t) = z(0,t) = 0 \tag{S2e}$$

such that parasites castrate their hosts (i.e. $f_y(a) = f_z(a) = 0$) and all age-0 individuals are born uninfected. As initial conditions we consider

$$x(a,0) = x_d(a) \tag{S2f}$$

$$y(a,0) = z(a,0) = 0 \tag{S2g}$$

such that the initial age distribution of the population consists entirely of uninfected individuals. Besides considering age and time distinctly, model (S2) therefore differs from our model of the main text by including a birth rate for age-0 individuals and a mortality rate for uninfected individuals.

Discretization

Model (S2) is written as a system of partial differential equations but we implement it numerically through a discretization of age, relying on a sufficiently small age increment to achieve accuracy in the approximation. More specifically, we discretize the host population into $s = 1001$ age-stages and use an age increment of $da = 0.1$. The maximum age of individuals is thus $a_+ = (s-1)da = 100$ and we describe the dynamics of the uninfected and two parasite-infected host types by a system of $3s$ ordinary differential equations. The density dynamics of the age-0 individuals of each host type are therefore described by

$$\frac{dx_0(t)}{dt} = -\mu_x(0)\; x_0(t) - x_0(t)/da + \sum_{i=0}^{s} x_i(t)\; f_x(i \cdot da) \tag{S3a}$$

$$\frac{dy_0(t)}{dt} = -\mu_y(0)\; y_0(t) - y_0(t)/da \tag{S3b}$$

$$\frac{dz_0(t)}{dt} = -\mu_z(0)\; z_0(t) - z_0(t)/da\,, \tag{S3c}$$

and the dynamics of all other $i \in 1, 2, \ldots, s$ age-stages are described by

$$\frac{dx_i(t)}{dt} = -\mu_x((i-1)\cdot da)\; x_{i-1}(t) - (x_i(t) - x_{i-1}(t))/da \tag{S3d}$$

$$- \lambda_y((i-1)\cdot da)\; x_{i-1}(t) - \lambda_z((i-1)\cdot da)\; x_{i-1}(t) \tag{S3e}$$

$$\frac{dy_i(t)}{dt} = -\mu_y((i-1)\cdot da)\; y_{i-1}(t) - (y_i(t) - y_{i-1}(t))/da \tag{S3f}$$

$$+ \lambda_y((i-1)\cdot da)\; x_{i-1}(t) + \lambda_y((i-1)\cdot da)\; z_{i-1}(t) \tag{S3g}$$

$$\frac{dz_i(t)}{dt} = -\mu_z((i-1)\cdot da)\; z_{i-1}(t) - (z_i(t) - z_{i-1}(t))/da \tag{S3h}$$

$$+ \lambda_z((i-1)\cdot da)\; x_{i-1}(t) - \lambda_y((i-1)\cdot da)\; z_{i-1}(t)\,. \tag{S3i}$$

Scenarios & Results

We implemented model (S3) in *Mathematica* v13.0 using the "ExplicitEuler" integration method of `NDSolve` with a step size of da to investigate the same sets of scenarios considered in Fig. 1 of the main text:

1. an *age-independent force-of-infection that varies by parasite* with an age-independent mortality rate that is not affected by infection (Fig. S1a);

2. an *age-dependent force-of-infection that varies by parasite* with an age-independent mortality rate that is not affected by infection (Fig. S1b);

3. an *age-independent infection-induced mortality that varies by parasite* with an age-independent force-of-infection that does not vary by parasite (Fig. S1c); and

4. an *age-dependent infection-induced mortality that varies by parasite* with an age-independent force-of-infection that does not vary by parasite (Fig. S1d).

For the second set of scenarios we describe the age-dependent force-of-infection rates as being linearly proportional to host age (e.g., $\lambda_y(a) = \beta_{0(\lambda_y)} + \beta_{1(\lambda_y)}\; a$). For the fourth set

of scenarios we describe the age-dependent mortality rates to either be an increasing function of host age (e.g., $\mu_y(a) = \beta_{0(\mu_y)}(1 - \exp^{-\beta_{1(\mu_y)}a})$) or a decreasing function of host age (e.g., $\mu_y(a) = \beta_{0(\mu_y)}(\exp^{-\beta_{1(\mu_y)}a})$), choosing these functions because they are bounded to be above zero and share the same maximum possible value of $\beta_{0(\mu_y)}$.

For all scenarios we assume for simplicity that the mortality rate of uninfected individuals is an age-independent constant (i.e. $\mu_x(a) = \mu_x = 0.01$), that only uninfected individuals of at least age 10 have a non-zero age-independent fecundity

$$f_x(a) = \begin{cases} 0.1 & \text{for } a \geq 10 \\ 0 & \text{for } a < 10\,, \end{cases} \tag{S4}$$

and that the initial age distribution $x_d(a)$ is uniform between the ages of 10 and 25. None of these assumptions or specifications affect the steady-state form of the two parasites' age-prevalence curves; they affect only the time-course of the system's transient dynamics. Parameter values for each investigated scenario are given in Table S1, corresponding to those given in Table 1 of the main text.

Table S1: Parameters used to simulate (S3) for each of the four sets of scenarios corresponding to the four panels of Fig. S1. β_1 entries of '-' indicate age-independence. The values of additional parameters kept constant across all scenarios are given in the text.

Scenario	Force-of-infection				Mortality				Line color
	$\lambda_y(a)$		$\lambda_z(a)$		$\mu_y(a)$		$\mu_z(a)$		
	β_0	β_1	β_0	β_1	β_0	β_1	β_0	β_1	
(a) *Force-of-infection varies by parasite* (Fig. S1a)									
1	0.01	-	0.01	-	0.01	-	0.01	-	purple
2	0.005	-	0.02	-	0.01	-	0.01	-	teal
3	0.02	-	0.005	-	0.01	-	0.01	-	yellow
(b) *Force-of-infection varies by host age and parasite* (Fig. S1b)									
1	0	0.001	0.01	-	0.01	-	0.01	-	teal
2	0.01	-	0	0.001	0.01	-	0.01	-	yellow
(c) *Infection-induced mortality varies by parasite* (Fig. S1c)									
1	0.01	-	0.01	-	0.05	-	0.02	-	teal
2	0.01	-	0.01	-	0.02	-	0.05	-	yellow
(d) *Infection-induced mortality varies by host age and parasite* (Fig. S1d)									
1[a]	0.01	-	0.01	-	0.1	0.02	0.01	-	teal
2[b]	0.01	-	0.01	-	0.1	0.02	0.01	-	yellow

[a] Mortality rate *increasing* with age.
[b] Mortality rate *decreasing* with age.

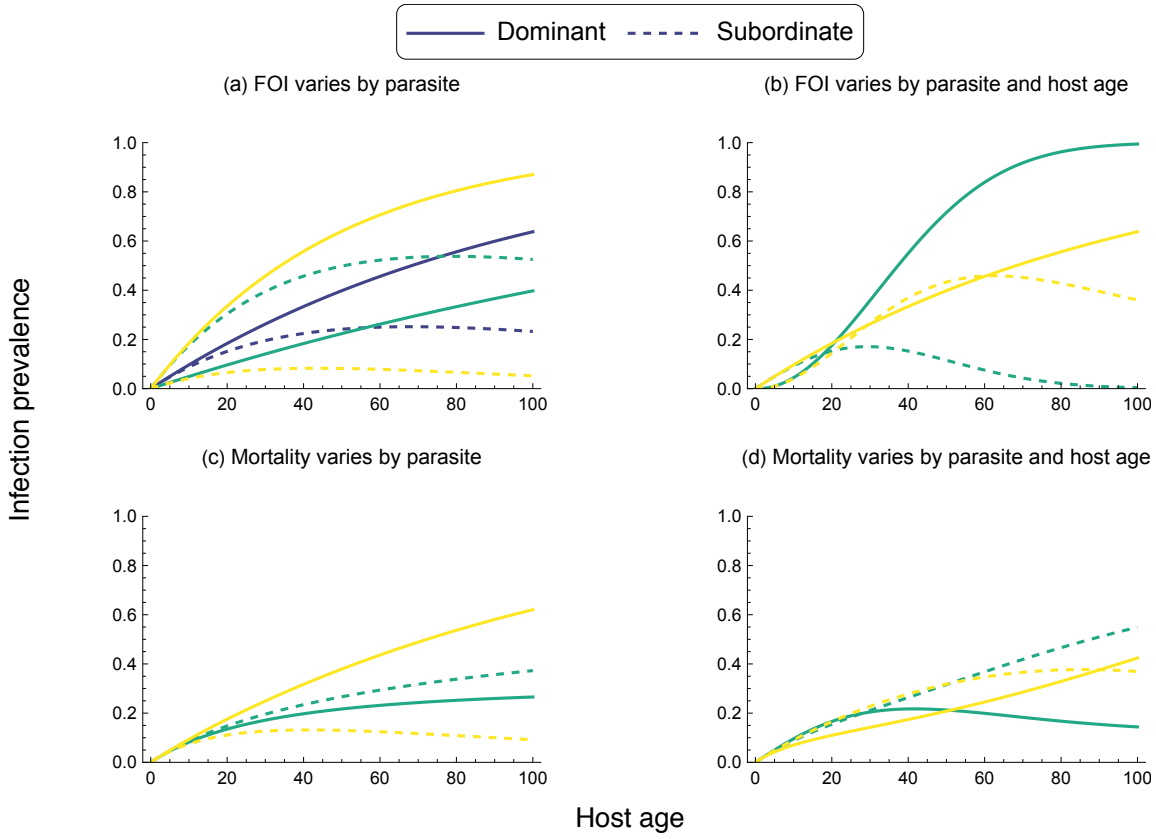

Figure S1: Corresponding to Fig. 1 of the main text, the steady-state age-prevalence curves of the dominant and subordinate parasite (at time $t = 200$) as simulated using (S3) for each of the four sets of scenarios detailed in Table S1.

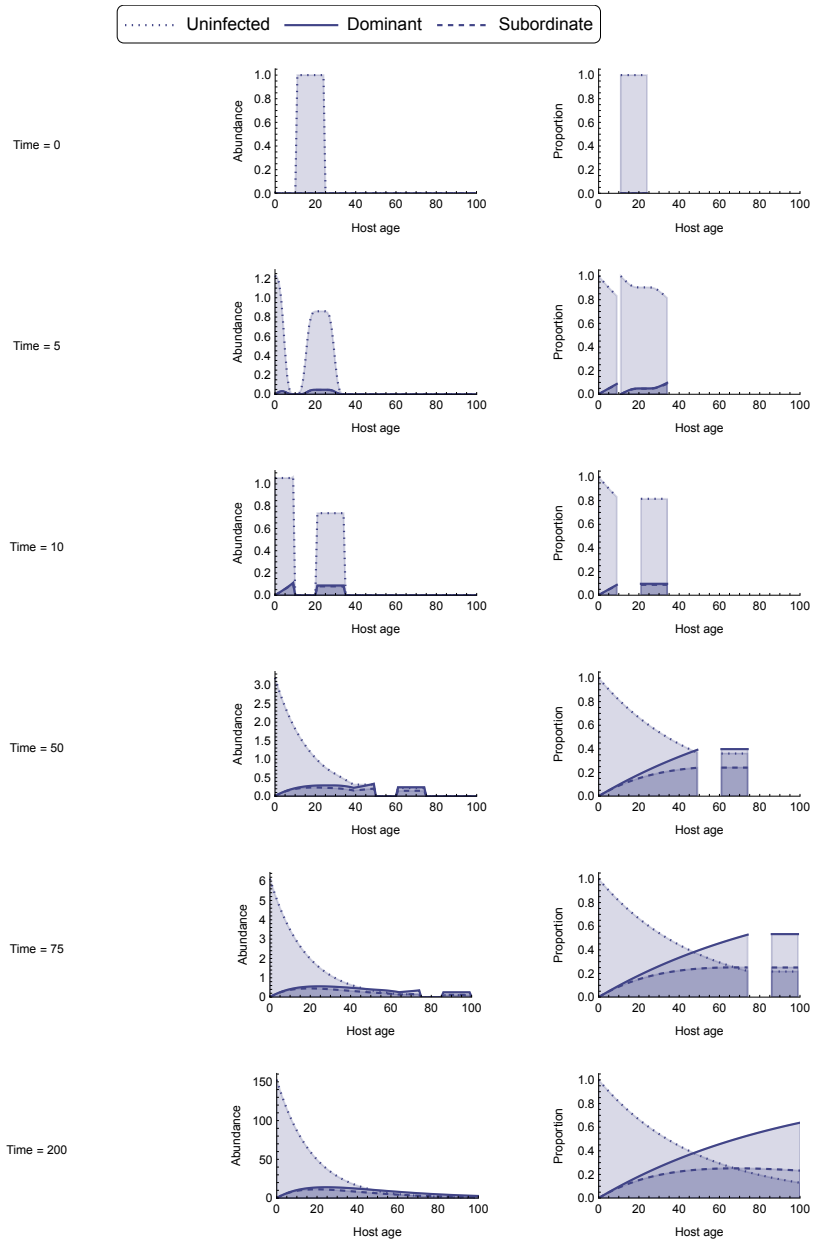

Figure S2: The transient dynamics of the host population over time for the purple baseline scenario of Fig. S1(a) and Table S1(a) in which the two parasites do not differ in their force-of-infection or their infection-induced mortality rates. The left-hand column depicts the densities of the three host groups while the right-hand column depicts their proportional abundances (i.e. age-prevalence curves). The initial population at time = 0 is comprised of only uninfected individuals distributed uniformly between the ages of 10 and 25. Age-0 individuals are only produced by individuals aged greater than 10, thus the illustrative initial gap of individuals less than age 10 is lost only as the first-born age-0 individuals replace all older individuals. Thereafter the transient dynamics give way to stable age-prevalence distributions.